

Chapter 4

Role and Prospects of Polymer-Based Nanomaterials in the Dielectric World



Sushrisangita Sahoo, Abhinav Yadav, K. P. Andryushin,
and L. A. Reznichenko

Abstract The development of reliable energy storage systems is the best strategy to resolve the global crisis of increased energy consumption in this modern high-tech world and exhaustion of fossil fuels for energy production. Electrostatic capacitors are one of the extensively used energy storage systems by the engineers and researchers among other such devices like supercapacitors and batteries due to its unique characteristics of superior charge density, ultrafast charge and discharge, high stability, and long-life time. These unique features made them suitable for distributed power systems, microelectronic circuits, electric vehicles, etc. But these electrostatic capacitors have the demerits of low energy density. Therefore, the main objective of researchers is now to achieve high energy density and energy storage efficiency along with the high-power density. The only possible way to attain the high energy density of the electrostatic capacitor is to tailor the features of dielectric materials. Both the ceramics and polymers were used individually in the dielectric layer of the electrostatic capacitors, while the both the individuals have some pros and cons. So, materials scientist combines both the ceramics and polymer to obtain the pro qualities of polymer like high breakdown strength and flexibility, and high dielectric constant of ceramics. Recently, ceramics in nanoform are chosen as the filler materials to the polymer matrix in the trend of device miniaturization. So, in this chapter, we will discuss about the various attempts made to design the polymer-ceramic nanocomposites to obtain the high dielectric constant and hence the energy density of the material.

Keywords Nanocomposites · Polymer · Filler · Dielectric permittivity · Breakdown strength

S. Sahoo (✉) · A. Yadav · K. P. Andryushin · L. A. Reznichenko
Research Institute of Physics, Southern Federal University, 344090 Rostov-on-Don, Russia
e-mail: sushri1990@gmail.com; ssahoo@tuskegee.edu

S. Sahoo
Department of Material Science and Engineering, Tuskegee University, Tuskegee, AL 36088,
USA

4.1 Introduction

The current craze in portable and wearable electronics in the modern high-tech world triggered a growing interest of scientific communities toward the design and development of flexible piezo/triboelectric nanogenerators for energy harvesting and storage devices [1–4]. Polymer-based materials are the best option to choose as the base material for flexibility purpose as it can easily rollable, foldable, twistable, and bendable. Flexibility is not only the feature required for energy harvesting and storage devices, so we need to optimize other parameters for the device performance. On the other hand, we are all aware of the fact that the exhausted usage of fossil fuels and high consumption of energy in the modern high-tech world became a serious threat to our society. To avoid the consequences of this serious threat, we need to resolve these problems by (1) developing some cost-effective, ecofriendly, and efficient energy storage devices and (2) diverting our path from exhausting usage of nonrenewable energy resources to renewable energy sources (like wind, sun, sound thermal and mechanical energy, etc.). So, some of the researchers now put their efforts on energy conversion from environmental phenomena. Though the idea of energy conversion seems very simple, it is really challenging due to the intermittent nature of this energy sources [5–9]. Some other material researcher trying to resolve the storage of the conversion energy in a stable and controlled manner [10]. Among all the storage systems (such as flywheel energy storage, compressed air storage, and hydro storage), the electrochemical energy storage systems, fuel cells, and electrostatic capacitors are widely used by the researchers [11–13]. The two main subsystems of electrochemical storage systems are Li-ion batteries and supercapacitors, both depends on electrochemical processes to store energy, but both of them have different working mechanism yielding different charge storage properties [14]. However, the electrostatic capacitors usually store the energy through electric field induced polarization and depolarization process [15].

Li-ion batteries follow the diffusion controlled faradic reactions in the bulk electrode to store energy, i.e., the Li-ion travels from anode to cathode or cathode to anode during charging and discharging process, and hence, the process is slow [14]. The bulk storage mechanism of batteries causes its high energy density, whereas the lengthy process yields low power density and short life time. In contrast to batteries, supercapacitors stores energy either through the accumulation of electrostatic charge on the electrode–electrolyte surface (EDLC) or through fast and reversible redox reactions (pseudocapacitors) [16]. Supercapacitors exhibit high-power density and long-life span, but low energy density. In contrast to the above two electrochemical storage devices, the electrostatic (or dielectric) capacitors store energy through electric-field-induced polarization and depolarization process and have unique pro qualities of ultrahigh-power density, greater cycling stability, and long lifespan [17–19], but limited energy densities [20]. The energy density of these dielectric capacitors strongly depend on their dielectric permittivity and breakdown strength. Conventional dielectrics are either polymer or ceramics. Both of them have some merits and demerits for application purpose. The ceramics exhibit high

dielectric permittivity and thermal stability, but have demerits of poor flexibility and low breakdown strength. However, the polymers have good flexibility and breakdown strength, but have low dielectric permittivity. Therefore, polymer nanocomposites were proposed, which incorporate the individual's merits by dispersing nanofillers in the polymer matrix [21–24]. Various types of polymer matrix used for energy storage devices including both ferroelectric and conducting polymer such as poly(vinylidene fluoride) PVDF, poly(methylmethacrylate) (PMMA), polyetherimide (PEI), PVDF-based copolymers, polyimide (PI), polypyrrole (PPy), polyaniline (PANI), polyvinyl alcohol (PVA), and polytetrafluoroethylene (PTFE) [25–35]. The ultimate properties of the polymer nanocomposites are strongly affected or controlled by the features of nanofiller, nanofiller/polymer interfaces, interaction between the nanofillers, and spatial composite structure. Hence, it has been a great challenge for researchers to achieve simultaneous improvement in dielectric permittivity (dielectric and energy storage properties) as well as breakdown strength (mechanical properties). A continuous effort has been made by the material researchers to solve the technical challenges associated with the polymer nanocomposites and improve their performance by choosing the suitable types of fillers, surface modification, microstructure and alignment of filler, complex structures, etc., for the application perspective. Various parameters are designed such as the (1) selection of the polymer matrix, e.g., linear dielectric or ferroelectric polymers, in some cases even conductive polymer matrix was also chosen; (2) nanofillers with different electrical properties (conductor, semiconductor, and dielectric), shapes, size, and compositions; (3) surface engineering; (4) hierarchical structures with different orientation and morphology of fillers; (5) multilayered nanocomposites [36–41].

Though excellent reviews on polymer nanocomposites are summarized earlier, but the collective information regarding the fundamental mechanisms and the significance of dielectric properties of polymer nanocomposites for energy devices as well as the theoretical and experimental approach to explain the crucial parameters are discussed in this chapter. Section 4.2 covers the basic concepts of dielectric, i.e., dielectric polarization to understand the working mechanism of capacitive storage, the dielectric breakdown, and energy storage density. Section 4.3 covers the models for dielectric permittivity and breakdown strength, which are used to explain the experimental trend of the polymer nanocomposites. Section 4.4 describes the crucial parameters which affect the overall properties of the polymer nanocomposites. The last section describes the different attempts made by the researcher to enhance and optimize these crucial parameters for energy storage devices.

4.2 Some Basic Concepts of Dielectric Capacitors and Energy Storage

Dielectric capacitors stores energy through electric-field-induced polarization and depolarization process. Since polarization, breakdown, conduction, and dissipation strongly affect the different properties of a dielectric material, we have discussed these mechanisms for better understanding of the basic concepts.

4.2.1 Dielectric Polarization

Polarization mechanism can be explained based on the response of individual atoms, ions, and dipoles of a dielectric material under the action of external applied field. The dielectric material polarized through displacement of atoms, ions, or dipoles from their equilibrium position by the action of an external electric field causing electric dipole moment. Electronic, ionic, dipolar or orientational, and space charge polarizations are the four different types of polarization mechanisms. Electronic polarization is the response of individual atoms to the external applied electric field. Each material constitutes atoms, and there is a symmetric distribution of electronic cloud and nucleus resulting zero dipole moment in the absence of applied electric field. But these atoms can be polarized due to the displacement of the centers of electron cloud and nucleus under the action of electric field causing some nonzero dipole moment. Electronic polarization is observed in all dielectrics and exists up to optical frequency range (ultraviolet/visible), i.e., a very high frequency range due to involvement of electron. Similarly, the displacement of positive and negative ions from their equilibrium position results a net induced dipole moment under the influence of electric field, and the corresponding polarization is called as the ionic polarization. Ionic polarization is observed in those dielectric materials which have ionic bonding and exists up to infrared frequency. But some dielectrics possess some permanent dipole moments, and the application of electric field causes these dipole moments to align in one direction. Such kind of polarization is called orientational polarization. Orientational or dipolar polarization is observed in polar dielectrics and exists only up to microwave frequency due to slow response of dipoles to the applied field. Due to electrical inhomogeneity, defects, and imperfections in some inhomogeneous dielectric material, charges are accumulated on the surfaces of grain and grain boundary or near the electrode interfaces resulting space charge or interfacial polarization. The total polarization of the dielectric material is the contribution of all these four types of polarization [20, 42].

4.2.2 Dielectric Breakdown

Breakdown suggests about the failure of a dielectric material against a certain applied electric field which causes the loss of its insulating properties and the corresponding electric field called as the breakdown strength or dielectric strength of the material. The breakdown process of the dielectric material involves three mechanisms such as electromechanical breakdown, intrinsic breakdown, and thermal breakdown. The dominance of electrostatic compressive force over the mechanical compressive strength is the main reason for electromechanical breakdown of the dielectric material. The breakdown strength of electromechanical breakdown is generally expressed in terms of Young's modulus (Y) as [43, 44]:

$$E_b = 0.606 \sqrt{\frac{Y}{\epsilon_0 \epsilon_r}} \quad (4.1)$$

The crossover of charge carriers (mainly electrons) from valence band to conduction band under the influence of very high electric field results large conduction currents and hence breakdown of dielectric material. This breakdown is known as intrinsic breakdown. The collision of highly accelerated electrons with atoms or molecules broke their covalent bonds under the application of high field and released more electrons and holes. This leads to a dielectric breakdown in a material, and it is known as avalanche breakdown. The thermal breakdown generally occurs in the dielectric material, when the heat produced through the conduction and leakage loss of the dielectric exceeds the dissipation of those energy through radiation and conduction.

4.2.3 Energy Storage

The energy density of polar or nonlinear dielectric materials can be defined as the integral of electric field (E) with respect to the electrical displacement (D) vector between the limit of remnant polarization (P_r) and maximum electrical displacement (D_{\max}) i.e. [19, 45],

$$U_e = \int_{P_r}^{D_{\max}} E dD \quad (4.2)$$

and the energy storage efficiency (η) can be defined in terms energy density (U_e) and energy loss (U_l) as the following equation:

$$\eta = \frac{U_e}{U_e + U_l} \quad (4.3)$$

The energy loss (U_l) represents the energy dissipated during the charge and discharge process of dielectric material. U_l also denotes the (1) energy consumption of all the dielectric materials during polarization and depolarization process and (2) unavoidable leakage loss.

The electrical displacement vector for these polar dielectrics can be expressed as:

$$D = P + \varepsilon_0 E \quad (4.4)$$

However, the energy density (U_e) for nonpolar or linear dielectric materials can be defined as the product of electrical displacement vector and electric field with some constant (i.e., $\frac{1}{2}$).

$$U_e = \frac{1}{2} DE \quad (4.5)$$

The electrical displacement vector for these nonpolar dielectric materials directly proportional to electric field and can be written as:

$$D = \varepsilon E = \varepsilon_0 \varepsilon_r E \quad (4.6)$$

ε_r , ε , and ε_0 are the relative dielectric constant and dielectric constants in medium and free space, respectively.

So, the above equation of energy density is deduced to [46, 47]:

$$\therefore U_e = \frac{1}{2} \varepsilon_0 \varepsilon_r E^2 \quad (4.7)$$

All these mathematical expressions clearly indicate the significant contribution of these critical parameters such as polarization, dielectric constant, breakdown strength, and energy loss to the energy density of the dielectric material. Any one of them can affect the energy storage performance of the material. High dielectric constant and high breakdown strength are required to obtain high energy density of nonpolar (linear) dielectric material. Similarly, high polarization (or high dielectric displacement) and high breakdown strength are required for high energy density of polar (or nonlinear) dielectric material. High dielectric constant is needed for high polarization in polar dielectrics. Therefore, dielectric constant and breakdown strength are most important parameter, and their value should be high to obtain enhanced energy density for both polar and nonpolar dielectrics. On the other hand, it is not only to achieve the high energy density, but we have to optimize the energy storage efficiency. So, the dielectric material should have low energy loss, leakage loss, and conductivity. Polymer nanocomposites incorporate the individual's pro factor such as high breakdown strength of polymer and filler's high dielectric constant (or polarization) to optimize the most essential factor energy density and consequently the dielectric energy storage performance. The high dielectric

constant of these polymer nanocomposites can be obtained either from percolation polymer nanocomposites by addition of conductive fillers or from dielectric-reinforced polymer nanocomposites having intrinsic dielectric properties. Similarly, the breakdown strength has equal significance in energy storage, so the breakdown processes are also discussed in our following sections.

4.3 Models for Dielectric Permittivity and Breakdown Strength

As we have mentioned earlier, the polymer nanocomposites combined the pro quality of individual components such as the fillers which significantly contributes to the dielectric properties and the polymer matrix which provides the mechanical properties. The electrical properties of polymer nanocomposites exhibit completely different trends than the pure polymer and filler constituents. Therefore, several models are proposed to explain the dielectric properties of these polymer nanocomposites.

4.3.1 Models for Dielectric Permittivity

Initially, simple models such as series and parallel models are proposed by assuming continuous medium of polymer matrix with dielectric permittivity ' ε_p ' filled with spherical fillers of dielectric permittivity ' ε_f ', and both the filler and the polymer have no dielectric loss. The series and parallel model can be mathematically expressed as:

$$\text{Series Model : } \varepsilon_c = \frac{\varepsilon_p \varepsilon_f}{\varepsilon_p f_f + \varepsilon_f f_p} \quad (4.8)$$

$$\text{Parallel Model : } \varepsilon_c = \varepsilon_p f_p + \varepsilon_f f_f \quad (4.9)$$

where ε_c is the permittivity of the polymer composites, f_p and f_f represent the volume fraction of the polymer matrix and the filler, respectively.

Then, these simple models are modified by Sillars and Landau–Lifshitz which holds good for lower volume fraction of the filler, but limited to the conductivity of both filler and polymer matrix. The mathematical expression can be written as:

$$\varepsilon_c = \varepsilon_p \left[1 + \frac{3f_f(\varepsilon_f - \varepsilon_p)}{2\varepsilon_p + \varepsilon_f} \right] \quad (4.10)$$

Maxwell–Garnet equation which is more accurate than the previous ones but have the limitation in resistivity of polymer matrix and filler can be expressed as [48, 49]:

$$\varepsilon_c = \varepsilon_p \left[1 + \frac{3f_f(\varepsilon_f - \varepsilon_p)}{(1 - f_f)(\varepsilon_f - \varepsilon_p) + 3\varepsilon_p} \right] \text{ (For spherical fillers)} \quad (4.11)$$

and

$$\varepsilon_c = \varepsilon_p \left[1 + \frac{f_f(\varepsilon_f - \varepsilon_p)}{A(1 - f_f)(\varepsilon_f - \varepsilon_p) + \varepsilon_p} \right] \text{ (for non spheroid fillers)} \quad (4.12)$$

$A = \frac{1}{3}$ is the depolarization factor, which indicates the deviation from spherical shape of the dispersed filler.

Then, Bruggeman proposed an improved model (expressed in the following equation) which is valid for relatively large volume fractions of spherical filler than the previous models and for agglomerated or closely packed filler particles.

$$\varepsilon_c = \varepsilon_f \frac{3\varepsilon_p + 2f_f(\varepsilon_f - \varepsilon_p)}{3\varepsilon_f - f_f(\varepsilon_f - \varepsilon_p)} \quad (4.13)$$

And the final Bruggeman equation can be written as [48, 50]:

$$\frac{(\varepsilon_f - \varepsilon_c)}{\varepsilon_c^{1/3}} = \frac{(1 - f_f)(\varepsilon_f - \varepsilon_p)}{\varepsilon_p^{1/3}} \quad (4.14)$$

Further, Jaysundere and Smith proposed a model by considering the interaction between the filler particles which cannot be neglected for nanosized fillers and also in large volume fractions of filler, hence, calculated the overall electric field by including the polarization of adjacent particles. This factor was neglected in previous models as all of them are valid for lower filler loadings and assumed less interaction of filler particles due to large distance between them. The Jaysundere–Smith equation can be written as [48, 51, 52]:

$$\varepsilon_c = \frac{\varepsilon_p f_p + \varepsilon_f f_f \frac{3\varepsilon_p}{(2\varepsilon_p + \varepsilon_f)} \left[1 + 3f_f \frac{(\varepsilon_f - \varepsilon_p)}{(2\varepsilon_p + \varepsilon_f)} \right]}{f_p + f_f \frac{3\varepsilon_p}{(2\varepsilon_p + \varepsilon_f)} \left[1 + 3f_f \frac{(\varepsilon_f - \varepsilon_p)}{(2\varepsilon_p + \varepsilon_f)} \right]} \quad (4.15)$$

Lichtenker proposed a model by modifying the initial idea of series and parallel model and calculated the formula for effective dielectric permittivity and conductivity of the polymer-based composites. The series and parallel models explained the lower and upper bound of the effective dielectric permittivity based on arrangement of the parallel layers of the composite perpendicular or along the field, respectively. The Lichtenker formula widen the lower and upper limit of the effective dielectric permittivity and can be written as [52, 53]:

$$\varepsilon_{\text{eff}}^\alpha = \varepsilon_p f_p^\alpha + \varepsilon_f f_f^\alpha \quad (4.16)$$

α is the parameter whose value explains the transition from anisotropy ($= -1$) to isotropy ($= 1$).

Another model was proposed to explain the dielectric properties of the polymer composite having conducting fillers and called as percolation model. Though insulating (inorganic) fillers mainly dispersed in polymer matrix to enhance the dielectric permittivity of the composite, the dielectric constant is not still high enough in application point of view even at high filler concentration and the high filler inclusion affects the mechanical properties of the host polymer. So, some researcher dispersed conducting fillers to achieve high dielectric constant of the composites. The high dielectric constant in these composites is the result of Maxwell–Wagner polarization. These composites also exhibit high loss and conductivity. Both the dielectric constant and conductivity of these composites follow a nonlinear trend above percolation threshold (f_c) which cannot be explained by the above-mentioned models. The equations for percolation theories can be written as [48, 49, 54]:

$$\varepsilon_c \propto (f_c - f_f)^{-q} \text{ for } f_f < f \quad (4.17)$$

$q = 0.8 - 1$ is the dielectric critical exponent.

Yamada model was proposed for polymer composites with higher loading of dielectric filler and the equation can be written as [55, 56]:

$$\varepsilon_c = 1 + \frac{\eta f_f (\varepsilon_f - \varepsilon_p)}{\eta \varepsilon_p + (\varepsilon_f - \varepsilon_p)(1 - f_f)} \quad (4.18)$$

η is the shape factor.

Yu et al. [56] fitted the experimental data of surface-modified BaTiO₃ nanofillers dispersed PVDF matrix composites with the Yamada model and find that the model simulation fitted well with the trend of experimental data of permittivity except the filler concentration at 60%.

Modified Kernel model was another model purposed which considers the interaction between the adjacent fillers in the polymer composites and the equation can be written as [53, 57]:

$$\varepsilon_c = \frac{\varepsilon_p f_p + \varepsilon_f f_f \left[\frac{3\varepsilon_p}{\varepsilon_f + 2\varepsilon_p} \right] \left[1 + \frac{3f_f(\varepsilon_f - \varepsilon_p)}{\varepsilon_f + 2\varepsilon_p} \right]}{f_p + f_f \left[\frac{3\varepsilon_p}{\varepsilon_f + 2\varepsilon_p} \right] \left[1 + \frac{3f_f(\varepsilon_f - \varepsilon_p)}{\varepsilon_f + 2\varepsilon_p} \right]} \quad (4.19)$$

4.3.2 Models for Breakdown Strength

Phase-field model, finite element simulation, stochastic simulation, and machine learning are the different type of breakdown simulations used to understand the dielectric breakdown mechanism of the polymer nanocomposites.

Dielectric breakdown model:

The dielectric breakdown model was proposed to understand the underlying mechanism of breakdown patterns in a polymer composite by assuming the homogeneous distribution of the dielectric fillers in the polymer matrix. The formed electrical trees in the polymer composite propagate through the dielectric medium during the dielectric breakdown, and the electrical field affects this tree channel growth. So, the mathematical relation between the probability (p) of tree channel growth and the electric field (E) can be expressed as [58]:

$$p(i, k \rightarrow k', k') = \frac{(E_{i,k'})^\eta}{\sum (E_{i,k'})^\eta} \quad (4.20)$$

where η is the exponent and i, k' represents the tree channel growth sites.

Failure probability and fractal dimension are the two factors which can determine the electrical tree behaviors. The number of channels connected to the electrical tree are controlled by the factor called propagation time, which affect the failure probability. Similarly scaling behavior (C) is another function used to calculate the fractal dimension (D) using the following mathematical relation:

$$C_r = C_0 r^{D-2} \quad (4.21)$$

where r represents the radius of the circle which covers all the electrical sites.

The failure probability was also explained on the basis of Weibull distribution model. The Weibull statistics model can be mathematically expressed as [45, 59, 60]:

$$P = 1 - e^{-\left(\frac{E}{E_0}\right)^\beta} \quad (4.22)$$

where P , E , E_0 , and β represent the cumulative probability of electric failure, experimental breakdown data, scale parameter, and shape parameter, respectively. The scale parameter suggests the field strength where there is a 63% probability for the sample to breakdown (characteristic E_b), and the shape parameter called as the Weibull modulus displays the dispersion of E .

Modified dielectric breakdown model:

The dielectric breakdown model was again modified for randomly distributed filler in the polymer matrix by introducing a new term “ L_i ” in the existing equation of

probability as [58]:

$$p(i, k \rightarrow k', k') = \frac{\left(\frac{E_{i,k'}}{L_i}\right)^\eta}{\sum \left(\frac{E_{i,k'}}{L_i}\right)^\eta} \quad (4.23)$$

where L_i was represented as the pertaining breakdown channel length which can be expressed as:

$$L_i = L_0 - \frac{L_0}{a_i} \quad (4.24)$$

a_i is the distance between the conducting particle.

Wang et al. used the modified dielectric breakdown model to explain the improvement of breakdown strength of a sandwich polymer nanocomposites which constitute an array of ultrasmall metal particles (Ag, Au, or Pt) in between the layers of PVDF HFP.

Phase-field model:

Ceramics or dielectric fillers with high dielectric constant were dispersed in the polymer matrix to enhance the effective dielectric permittivity of the polymer nanocomposites. The accumulation of charges in the interfaces of ceramic fillers and the polymer matrix due to the huge difference in their dielectric constant also affects the local electric field at the interface and consequently deteriorates the breakdown strength of the polymer nanocomposites. Further, application of electric field above a critical value may initiate cracks and weak paths to propagate, resulting in a complete breakdown. Phase-field model was developed to describe the damage initiation and the progress in the polymer composites [61]. The dielectric breakdown of the polymer composites can be explored by obtaining the local field distributions and crack propagation details continuum phase-field model [62]. The influence of microstructure on the breakdown strength, energy density, and dielectric permittivity of the polymer composites can also be investigated from the simulation of this model. This model can also design the novel microstructures of desired energy density and breakdown strength. The influence of various stimuli (e.g., mechanical, electrical, and thermal stimulus) on breakdown behavior of polymer composites can be predicted by the continuous phase-field model. By considering the contribution of electric energy, phase separation energy, and gradient energy, one can develop the phase-field model to simulate the breakdown strength in polymer nanocomposites. The contribution of thermal energy which was not included in the phase-field model was incorporated to develop the electrothermal breakdown model, which predicts well about the breakdown strength of the 3D filler-based polymer nanocomposites.

Stochastic model:

Stochastic model was proposed to understand the breakdown phenomena by studying one of the most important features, i.e., the fractal properties of the branched

discharges. According to this model, the growth probability depends on the local field (potential), and the mathematical expression can be written as [63]:

$$p(i, k \rightarrow i', k') = \frac{(\varphi_{i',k'})^\eta}{\sum (\varphi_{i',k'})^\eta} \quad (4.25)$$

The denominator represents all the possible growth processes.

Yue et al. [64] reported a modified stochastic model to study the growth of the breakdown path and the internal electric field distribution of the polymer composites under the applied electric field. The break down probability $P(r)$ was reported as:

$$P(r) = \frac{E(r)^2}{E_b(r)^2} / \sum \frac{E(r)^2}{E_b(r)^2} \quad (4.26)$$

where $E(r)$ and $E_b(r)$ represent the electric field of a local point and intrinsic breakdown strength, respectively. The denominator suggests the sum of all points where local electric field exceeds the breakdown strength. In addition to modified stochastic model, they also used the machine learning to study the breakdown strength of the polymer composites. They used three parameters, i.e., the dielectric permittivity, size, and content of the filler, to build the model for the breakdown process of the polymer composites.

Finite element simulations:

Wang et al. [65] investigated the local electric field distribution and its effect on breakdown strength of the polymer composites by finite element simulations, when high permittivity fillers like barium titanate were added on the polymer matrix. Similarly, the local field distributions and leakage current density of the double-layered composite of boron nitride surface-modified BCZT ferroelectric nanofillers and PVDF polymer were analyzed by the finite element simulations [66]. The electric field distribution in the layered structure of PVDF/PMMA polymer composites was analyzed from the finite element analysis [67]. The effect of surface-modified barium titanate nanoparticle by TiO_2 and polydopamine filler on breakdown strength of epoxy composite was studied by finite element simulations [68].

4.4 Crucial Parameters (Dielectric Permittivity, Dielectric Loss, Breakdown Strength, and Energy Density) of Polymer-Based Nanocomposites

The first crucial factor in polymer composite dielectric is the type of dielectric material which means the variation of electric displacement is different in different dielectric materials with application of electric field as the polarization and energy loss is different in polar and nonpolar (linear) dielectrics. There are mainly two types of

dielectrics: (1) polar or nonlinear dielectrics and (2) nonpolar or linear dielectrics. Again, the polar or nonlinear dielectric subcategorized to ferroelectric (both normal and relaxor) and antiferroelectric. However, the nonpolar dielectrics include the linear dielectrics and paraelectric material. The variation of electric displacement for both polar and nonpolar dielectrics with application of electric field is illustrated in Fig. 4.1. It is clear from the figure that the nonlinear dielectrics have more pronounced energy loss, but they also exhibit high polarization and dielectric constant. Relaxor ferroelectric material possess high saturation polarization, low remnant polarization, and moderate breakdown strength, which made them potential material among all the dielectric. The efficiency of these relaxor materials can reach up to 90%, and the narrow hysteresis loop suggests the low energy dissipation in the form of heat during discharging. As we have mentioned in our previous Sect. 4.2.3, the energy storage density and efficiency of these polar dielectrics depend upon the remnant polarization and saturation polarization and low energy loss. However, the linear dielectrics (e.g., polymers or some composite) exhibits almost no energy loss, but their energy density was limited due to their low polarization and dielectric permittivity.

From the above discussion on energy density of capacitive storage, we found that the other important parameters are the dielectric permittivity and breakdown strength. Various types of nanofillers based on their electrical properties like dielectric/ceramics, conducting, and semiconducting are incorporated in the polymer matrix to improve the dielectric permittivity of the polymer nanocomposites. More details regarding the inclusion of ceramics, conductive and semiconductive nanofillers for the enhancement of dielectric permittivity, and the energy storage properties are discussed in or following sections. However, in search for high permittivity of the polymer nanocomposites, researchers never tried to sacrifice the flexibility of the

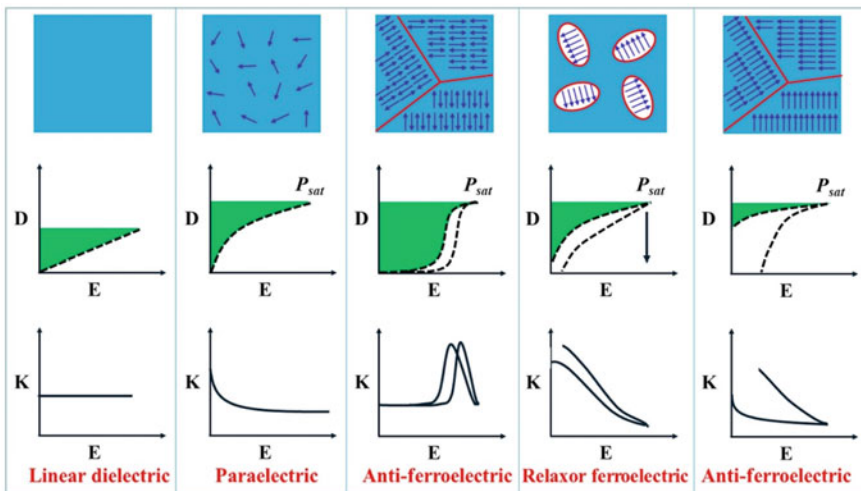


Fig. 4.1 Variation of electric displacement with applied electric field in linear and nonlinear dielectric. Reprinted with permission from Ref. [69]. Copyright 2019 Elsevier

polymer matrix. So, a small amount of filler incorporated in the polymer matrix to maintain the flexibility. In case of linear dielectrics, there is only induced polarization; whereas for polymer nanocomposites, the total polarization is the contribution of polarization of the nanofiller, the interaction between the fillers, and interface between the polymer matrix and nanofillers. The inclusion of nanofiller (whether it is conductive or insulating) in polymer matrix has a significant effect on overall properties of the polymer nanocomposites because the large surface area of nanomaterials create a large interaction zone among the nanofiller and the polymer matrix. In addition, the inclusion of nanofiller also changes the surface morphology of the polymer matrix. The small size of the nanofiller also modifies the internal field and space charge distribution of the polymer nanocomposites. The space charge distribution and the scattering effect due to the incorporation of nanofillers significantly affect the breakdown strength and dielectric permittivity of the polymer nanocomposites. Maxwell–Wager–Sillars theory was used to explain the interfacial space charge behavior of polymer nanocomposites [70]. Two different models, i.e., Lewis and Tanaka's model [71–73], are purposed to understand the effect of interface due to inclusion of nanosized filler in the polymer matrix, and the details of models, the influence of interface in different parameters, and overall properties of the composites are explained in Prateek et al. They also reviewed in detail the effect of (i) shape of conducting and nonconducting filler with different dimensions (0D, 1D, 2D), (ii) the 1D and 2D fillers with different aspect ratios on overall properties of the polymer nanocomposites. Another important parameter in the energy density equation is the breakdown strength, but it was studied that the enhancement of breakdown strength always accompanied by the decrease in dielectric permittivity. The inverse relationship between the breakdown strength and dielectric permittivity mainly attributed to the local electric field distribution in the polymer nanocomposites due to huge difference of individual dielectric permittivity of filler and matrix. We can neither ignore the breakdown strength nor the contribution of dielectric permittivity to the energy density, so we have to maintain these two parameters to obtain the optimized properties of the polymer nanocomposites. So, the one promising way to maintain these parameters is to reduce the difference of permittivity of filler and polymer matrix, and this can be obtained by adopting surface engineering, interfacial, and topological design. The examples of surface modification to maintain the breakdown strength of the polymer composites are discussed in the following section.

4.5 Different Approaches for Performance Improvement of Polymer Nanocomposites

(a) By adding different types of fillers in polymer dielectric

Different types of nanofillers such as conductors, semiconductors, and ceramics with different electrical properties are dispersed with the polymer matrix to tailor the dielectric and energy storage performance of the polymer nanocomposites.

Ceramics Fillers:

The most traditional way to achieve the high dielectric constant in the polymer nanocomposites is to incorporate ceramics filler such as $\text{Pb}(\text{Zr}_{0.5}\text{Ti}_{0.5})\text{O}_3$ (PZT) [74], $\text{CaCu}_3\text{Ti}_4\text{O}_{12}$ (CCTO) [75], BaTiO_3 (BT) [76], $\text{Na}_{1/2}\text{Y}_{1/2}\text{Cu}_3\text{Ti}_4\text{O}_{12}$ (NYCTO) [77], $\text{Ba}_x\text{Sr}_{1-x}\text{TiO}_3$, $x\text{NaNbO}_3$ - $(1-x)\text{BaTiO}_3$ (NN-BT) [78], $(\text{Bi}_{0.5}\text{Ba}_{0.25}\text{Sr}_{0.25})(\text{Fe}_{0.5}\text{Ti}_{0.5})\text{O}_3$ (BFO–BST) [79], and $0.78\text{Bi}_{0.5}\text{Na}_{0.5}\text{TiO}_3$ – 0.22SrTiO_3 (BNT–ST) [80] in the polymer matrix. Some of other recent examples are also discussed in the following paragraph.

Considering ultrahigh dielectric and polarization response of the ferroelectric ceramics near the morphotropic phase boundary (MPB), Xie et al. [81] chosen the MPB composition of the $\text{Pb}(\text{Zr}_{0.52}\text{Ti}_{0.48})\text{O}_3$ (PZT) nanocubes (NCs) as ceramic fillers for the P(VDF–CTFE) polymer matrix. But, as we know, the huge difference between the dielectric constant of the PZT ceramic and the PVDF–CTFE polymer would cause accumulation of charges in the interfaces between the ceramic and polymer, which also affect the local electric field at the interface and consequently the reduction of overall breakdown strength of the polymer nanocomposite. Again, the high conductivity of the ferroelectric ceramics filler will induce the high leakage current and loss of the polymer nanocomposite and hence affect the energy density. So, to avoid such problems, they tried to introduce a buffer coating layer of SiO_2 over the PZT ceramics. The dielectric constant of the polymer nanocomposites increased from 11 of pristine polymer to 15.8 at 1 kHz in the addition of 5 vol% of the filler. This core–shell structure PZT@ SiO_2 embedded P(VDF–CTFE) nanocomposites possess a high energy density of 16.8 Jcm^{-3} at breakdown strength of 491 MVm^{-1} . Xie et al. [82] studied the effect of three different types of filler, i.e., semiconductive (SiO_2), conductive (Al_2O_3), and dielectric nanofiller (BaTiO_3) on dielectric and energy storage properties of polypropylene polymer matrix experimentally explained based on theoretical models and visualized simulation. Jaysundere–Smith, Maxwell–Wagner, and parallel models are used to explain the experimental data of the dielectric constant for all the composites. They found that the BaTiO_3 /PP composites are the best option to obtain high dielectric constant with low loss among the others by keeping the same breakdown strength for all the composites.

Conductive or Metallic Fillers:

Conductive fillers include the pure metallic nanoparticles, conducting polymers, and carbon-based nanoparticles like Fe_2O_3 [83], NiO [84], Ni, carbon black, W and Ag [85, 86] carbon nanotube [87, 88], graphene, etc., were used for the polymer nanocomposites [89–91].

The dramatic increase of dielectric constant near the percolation threshold leads to the development of conductive filler-based polymer composites. Qi et al. [92] explained clearly that the size of the metal filler has a significant effect on the properties of polymer composites. They also mentioned the relation between the percolation probability to the size ratio of the filler to composite thickness and proposed that the metal fillers in the nanometer range will be the suitable option for polymer composites for practical applications. They added Ag nanoparticles on the epoxy polymer

to form the metal-polymer nanocomposite which has the dielectric constant of 300 with a relatively low loss of 0.05. A highly aligned reduced graphene oxide (rGO)/epoxy polymer nanocomposites exhibit an exceptionally high dielectric constant of 14,000 with 3 wt% of the filler concentration at 1 kHz and explained on the basis of Maxwell–Wagner–Sillars polarization [93].

Semiconductor Fillers:

Apart from conducting and dielectric ceramics fillers, semiconducting nanofillers are also used to improve the dielectric constant of the polymer matrix and the enhanced dielectric constant in these semiconductor polymer nanocomposites is mainly observed near the percolation threshold. The pro qualities of semiconducting fillers include the appreciable band gap, low AC conductivity, relatively low dielectric constant compatible to the polymer matrix, and the nonlinear electrical characteristics.

The enhanced dielectric, energy storage performance of the semiconductor filler-based polymer nanocomposites, i.e., fullerene-type tungsten disulfide nanoparticle-PVDF, was recently reported by Guo et al. [94]. They observed the enhancement of polar electroactive phases with increase in filler content leading to enhanced dielectric, mechanical, and energy storage properties. The dielectric constant increases 1.5 to 4 times than the pristine polymer PVDF even in the moderate addition of filler, whereas the higher filler concentration exhibits dielectric constant more than 40 times with an increase in $\tan \delta$. The dielectric behavior with the filler content was explained with the percolation model and fitted with various model for the comparison as shown in Fig. 4.2.

Similarly, Jia et al. enhanced electrical polarization and improved dielectric constant of a semiconductor nanostructured filler (both flower and nanosheet) in the PVDF matrix [95]. A novel three-dimensional zinc oxide superstructures (flower and walnut like) filler was used by Wu et al. [96] to tailor the dielectric constant and breakdown strength of the PVDF polymer matrix. The polymer nanocomposites significantly enhance the dielectric constant to 19.4, 104.9, and 221.1 for commercial ZnO, walnut-like, and flower-like ZnO superstructures at 100 Hz, whereas their breakdown strengths are found to be 45, 40, and 42 kV/mm, respectively. Ji et al. [97] used nickel hydroxide $\text{Ni}(\text{OH})_2$ nanoparticles in three different dimensions, i.e., nanosphere (0D), nanoplates (1D), and nanoflowers (3D) as fillers in the PVDF matrix, and the existence of -OH group will enhance the polar/electroactive β phase of PVDF. The -OH group will act as a surface layer above the Ni and do not need additional surface modification of the conductive filler. The hydroxyl group will provide a good interaction between the polymer matrix and filler. The maximum energy density of 17.3 J/cm³ at 421 kV/mm and dielectric constant of 16.3 at 100 Hz were observed for 5 wt% nanoplates- $\text{Ni}(\text{OH})_2$ based composites in comparison with other nanofillers having different dimensions. It also suggests the filler dimension which also affects dielectric and energy storage properties. A semiconductor-based hybrid filler, i.e., $\text{ZnO}@\text{MoS}_2$ was used to modify the different properties of poly(vinylidene fluoride-chlorotrifluoroethylene-double bonds) [98]. The 2 wt% of this hybrid nanofiller (4 mol% of MoS_2 in ZnO) in the polymer matrix yields the

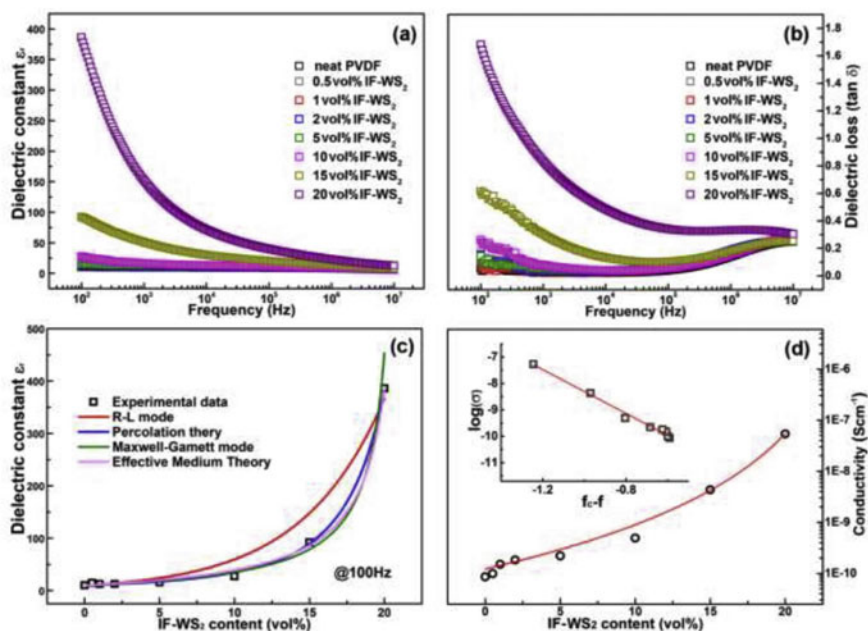


Fig. 4.2 Variation of dielectric constant with respect to frequency and filler content of fullerene-type tungsten disulfide nanoparticle-PVDF nanocomposites. Fitting of experimental data of dielectric constant with filler content by various model. Reprinted with permission from Ref. [94]. Copyright 2020 Elsevier

energy density of 7.2 Jcm^{-3} at 300 MVm^{-1} which is 70% higher compared to that of pristine polymer and possess high energy efficiency of 83%.

Jing et al. [99] prepared a polymer nanocomposite by incorporating a completely new type of filler, i.e., a high entropy oxide nanofiber ($\text{Eu}_{0.2}\text{Bi}_{0.2}\text{Y}_{0.2}\text{La}_{0.2}\text{Cr}_{0.2}\text{O}_3$) in the P(VDF-HFP)/PMMA polymer matrix. The 0.6 wt% of the filler concentration leads to highest breakdown strength of 509.4 kV mm^{-1} and energy density of 15.13 Jcm^{-3} . The enhanced breakdown strength in the nanocomposites is explained by the several factors such as polymorphic distortion caused by the high entropy in the lattice, and the movement of the long polymer was restricted by the pinning effect associated with the polymorphic distortion and reduces the loss in strong electric field and promotes the breakdown strength. The transmission of space charges is also blocked by the charge shielding layer between the nanofiber and the polymer, which again contributes to the enhanced breakdown strength.

Heterogenous fillers are also used in some literatures where both conductive and insulating fillers are used for the polymer nanocomposites. Ji et al. [100] used multi-walled carbon nanotube (MWCNTs) and barium titanate (BaTiO_3) fillers and PVDF polymer to prepare multilayered films with alternate distribution of layers. They also proposed a theoretical calculations/model for dielectric properties of heterogenous filler-based polymer nanocomposites by modifying the classical series model

by considering the contribution of two additional factors, i.e., filler distribution and interfacial polarization.

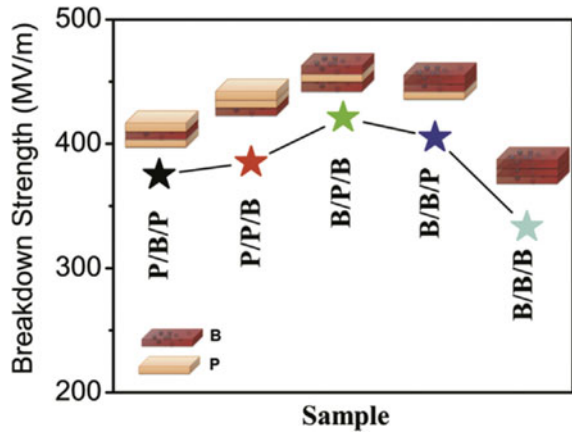
4.6 By Structural Design and Surface Engineering

Recently, Zeng et al. [101] developed a novel polymer nanocomposite by incorporating a surface-modified BaTiO₃ nanoparticle with polyimide (PI) polymer shells in the polyetherimide (PEI) polymer matrix. The dispersion of core-shell structured PI@BTO nanofillers yields an improved the energy density to 15.55 Jcm⁻³ with charger-discharge efficiency (η) of 80% and enhanced breakdown strength of 600.7 MVm⁻¹ in the PEI-PI@BTO nanocomposites. Similarly, Hu et al. [102] first designed a polymer nanocomposite by employing surface-modified core-shell nanofibers and then fabricated sandwiched structures by sandwiching these polymer nanocomposites layer in between the outer layer of host polymer matrix. They have chosen Ba(Ti_{0.85}Zr_{0.15})O₃ as core and Ba(Ti_{0.65}Zr_{0.35})O₃ as shell nanofibers for the core-shell structure, which was further modified by polydopamine (PDA). Then, after modification, they have added the surface-modified core-shell nanofiber to the PVDF polymer matrix in different filler concentration. Then, they fabricated three-layer sandwich structure by considering the polymer nanocomposite as the central layer in between the host PVDF outer layer. They observed the enhanced dielectric constant, breakdown strength, and energy density in lower filler content (2wt% of surface-modified core-shell structure) of both the single layer and trilayer nanocomposites. The energy density of the single and trilayer composites are found to be 8.2 and 9.9 Jcm⁻³, respectively. The energy density and breakdown strength of the polymer nanocomposites are tailored by adding different polymer@BaTiO₃ nanoparticle core-shell structure on PVDF HFP matrix in Li et al. [103]. The BaTiO₃ is surface modified by the polymethyl methacrylate (PMMA), polymethylsulfonyl ethyl methacrylate (PMSEMA), and polyglycidyl methacrylate (PGMA) polymers to prepare the core-shell structure. They studied the polarity of different polymer shell on the energy storage performance of the polymer nanocomposite and found the enhanced energy density and breakdown strength for the PMMA polymer shell with lowest polarity. Pan et al. [104] reported the enhanced dielectric constant of 149.5 at 1 kHz, high breakdown strength of 250.6 MV m⁻¹ with suppressed dielectric loss 0.19 of PVDF/MoS₂-PPy composites. The hybrid MoS₂-PPy nanofiller was fabricated by first exfoliating the molybdenum disulfide (MoS₂) with the cetyltrimethyl ammonium bromide (CTAB) solution and the exfoliated MoS₂ again followed by surface modification with conducting polymer polypyrrole (PPy). Xu et al. [68] recently reported a novel design of polymer nanocomposites by using a gradient dielectric filler means a double core-shell structure which not only improves the compatibility and dispersibility between the filler and polymer matrix but also improves the breakdown strength, nonlinear conductive, and dielectric properties. The double core-shell structure filler material constitutes BaTiO₃ nanoparticle as the core covered by TiO₂ as the first shell layer and then encapsulated by a second layer of polydopamine. Then,

this double core-shell structure filler was dispersed in the epoxy polymer matrix to prepare the polymer nanocomposites. Then, again these polymer nanocomposites were exfoliated boron nitride nanosheets with parallel and random alignments. The dispersion of this double core-shell structure filler with 10 wt% and the exfoliation of the polymer nanocomposite significantly improves the breakdown strength of the pure polymer matrix epoxy by 55%, i.e., from 29.4 to 45.7 kVmm⁻¹. The nonlinear trend of dielectric and conductivity properties of these nanocomposites were explained on the basis of nonlinear effective medium theory (EMT) and the hopping transport model, respectively.

Li et al. [105] developed sandwich-structured ceramic-polymer nanocomposites, which constitute BaTiO₃ nanofiber-(PVDF-HFP) composites as the outer layer and MgO nanowires-(PVDF-HFP) composites in the central layer in an objective to improve the breakdown strength and high dielectric constant by the outer layer and central layer, respectively. They found best energy density of 15.55 Jcm⁻³ and charge-discharge efficiency of 68% at Weibull breakdown strength of 416 MVm⁻¹ for the sandwich structure with 2 wt% MgO in the central layer and 20 wt% BaTiO₃ in the outer layers. Bai et al. [66] prepared a two-layer polymer composite, where the bottom layer constitutes the polymer composites of PVDF filled with boron nitride surface insulated 0.5(Ba_{0.7}Ca_{0.3})TiO₃-0.5Ba(Zr_{0.2}Ti_{0.8})O₃ (BCZT) nanofibers and the top layer consists of the boron-nitride-filled PVDF composite. They obtained a high breakdown strength and energy density by tailoring the ratios of boron nitrides in the top layer and also the amounts of surface-insulated BCZT nanofibers in the bottom layer. The PVDF-boron nitrides nanocomposite in the top layer exhibits an ultrahigh breakdown strength of 730 MVm⁻¹ for 0.8 wt% of fillers. The double-layer nanocomposites with the above composite in the top layer and the bottom layer with 1.6 wt% of BCZT@boron nitride nanofiber was found to be with energy density of 24.3 Jcm⁻³ at 718 MVm⁻¹. Luo et al. [106] designed a unique sandwich film in which the Ba_{0.6}Sr_{0.4}TiO₃ nanofibers network are completely interconnected and covered by the PVDF-HFP top and bottom layers. The sandwich film with 4 vol% of the nanofibers possesses an enhanced energy storage density of 9.46 J/cm⁻³, improved dielectric constant of 24.8 at 1 kHz and higher breakdown strength of 2954 kVcm⁻¹. Here, instead of polymer-based nanocomposites in the middle layer, a direct nanofiber network was used for the sandwich structure to improve the dielectric constant, energy density, and breakdown strength. Zhang et al. [67] reported high breakdown strength of 486.05 MVm⁻¹, energy density of 8.65 Jcm⁻³, and a high polarization of 4.48 μCcm⁻² for a sandwich structure of PMMA/PVDF blended layer (for 30 mass% of PMMA) covered by the outer layer of polyetherimide. The designing of different layered structures by ordering the polymer nanocomposites layer (called hard layer) and pure polymer layer (soft layer) in five different arrangements and the influence of interfaces between the adjacent layers on different parameters like breakdown strength and energy density were studied by Wang et al. [107]. The BaTiO₃/poly(vinylidene fluoride) nanocomposites represent the hard layer and denoted by B, and the pure PVDF layer represents the soft layer denoted by P. They observed the layer structure with polymer nanocomposites as the outer layer, and pure polymer in the middle layer (i.e., B-P-B film) exhibits

Fig. 4.3 Breakdown strengths of sandwich-structured films with different geometries. Reprinted with permission from Ref. [106]. Copyright 2021 Elsevier



the highest breakdown strength in comparison with others as shown in Fig. 4.3. They also prepared the single-layer polymer nanocomposites of PVDF and BaTiO₃ nanoparticles and compared the energy density and breakdown strength with the polymer nanocomposites. They found that both the energy density (7.02 Jcm⁻³) and breakdown strength (390 kVmm⁻¹) of layered structure are higher than those of single-layer nanocomposites.

4.7 Conclusion and Perspectives

In comparison with the recent energy storage systems such as supercapacitors, batteries, and fuel cells, dielectric capacitors attracted much attention of contemporary materials researcher due to its unique qualities such as high-power density, fast cycling rate, and long lifespan. But the application potentiality of conventional dielectric capacitors (either ceramics or polymer) is restricted by alternate pro qualities of pure polymer and ceramics, i.e., pure polymer's application potentiality is limited due to its low permittivity and energy density, whereas the ceramics lack in flexibility and breakdown strength. These shortcomings of conventional dielectric capacitors are resolved by fabrication of polymer-ceramics composites through inclusion of ceramics filler in the polymer matrix. Again, for further improvement in the energy storage properties with high energy density, polymer nanocomposites were developed which incorporates the fillers in nanoform (0D, 1D, 2D nanofillers). The main focus of the researchers in recent trend to design and develop efficient energy storage system is to optimize all the parameters of dielectric to attain high energy density and efficiency in polymer nanocomposites. The dielectric properties of the polymer nanocomposites strongly depend on the physical, chemical, and mechanical properties of both the fillers and polymer matrix. So, selection of both

the filler and polymer matrix is the most significant step to expect the desired parameters in the polymer nanocomposites. To obtain the high dielectric permittivity of the polymer nanocomposites, two different approaches have been made, i.e., addition of either (1) ceramics filler with high dielectric permittivity or (2) conductive filler associated with the percolation thresholds. But again, the addition of ceramics filler in the polymer matrix affects/deteriorates the breakdown strength of the polymer nanocomposites due to huge difference in their permittivity. So, to maintain both the breakdown strength and dielectric permittivity in polymer nanocomposites, surface modification of ceramics filler was carried out. Again, to reduce the difference of dielectric permittivity of polymer matrix and filler, conductive or semiconducting filler having comparatively lower permittivity was added to resolve the above issues. Both nanoparticles and nanofibers are added as fillers in the polymer matrix to prepare ternary composites with improved properties in comparison with binary composites. Novel structural design such as multilayered and core-shell structure has been developed to tailor the properties by interface minimization. Nanofillers (specifically 1D or 2D) with specific orientation or alignment found to be the best core filler in core-shell structured polymer nanocomposites to obtain enhanced dielectric constant. The difference in permittivity of polymer matrix and filler can be balanced by core-shell configuration and results a gradient dielectric permittivity. The development of different layered and laminated architecture also enables another way to improve in breakdown strength and energy density of the polymer nanocomposites.

Though there are many major breakthroughs in the design and development of polymer nanocomposites and tailoring their properties by novel approaches and architecture, still there are some unresolved quests to be explored in the future generation such as (1) the unsolved puzzle for simultaneous improvement breakdown strength and dielectric permittivity, (2) more attention needed to reduce the dielectric loss to improve the efficiency of energy storage, (3) new attempts and extensive analysis needed to alleviate the interfacial polarization, and (4) significant effort to design novel engineered architecture for effective energy storage systems.

Acknowledgements This research was funded by Ministry of Science and Higher Education of the Russian Federation: State task in the field of scientific activity, scientific project No. 0852-2020-0032 (BAZ0110/20-3-07IF).

References

1. Ghosh SK, Mandal D (2017) Bio-assembled, piezoelectric prawn shell made self-powered wearable sensor for noninvasive physiological signal monitoring. *Appl Phys Lett* 110:123701
2. Rahman W, Ghosh SK, Middy TR, Mandal D (2017) Highly durable piezo-electric energy harvester by a super toughened and flexible nanocomposite: effect of laponite nano-clay in poly(vinylidene fluoride). *Mater. Res. Express* 4:095305

3. Karan SK, Maiti S, Agrawal AK, Das AK, Maitra A, Paria S, Bera A, Bera R, Halder L, Mishra AK, Kim JK, Khatua BB (2019) Designing high energy conversion efficient bio-inspired vitamin assisted single-structured based self-powered piezoelectric/wind/acoustic multienergy harvester with remarkable power density. *Nano Energy* 59:169–183
4. Ding R, Zhange X, Chen G, Wang H, Kishor R, Xiao J, Gao F, Zeng K, Chen X, Sun XW, Zheng Y (2017) High-performance piezoelectric nanogenerators composed of formamidinium lead halide perovskite nanoparticles and poly(vinylidene fluoride). *Nano Energy* 37:126–135
5. Ryu H, Yoon HJ, Kim SW (2019) Hybrid energy harvesters: toward sustainable energy harvesting. *Adv Mater* 1:1802898
6. Vatansever D, Hadimani RL, Shah T, Siores E (2011) An investigation of energy harvesting from renewable sources with PVDF and PZT. *Smart Mater Struct* 20:055019
7. Karan SK, Maiti S, Agrawal DAK, Maitra A, Paria S, Bera A, Bera R, Halder L, Mishra AK, Kim JK, Khatua BB (2019) Designing high energy conversion efficient bio-inspired vitamin assisted single-structured based self-powered piezoelectric/wind/acoustic multienergy harvester with remarkable power density. *Nano Energy* 59:169–183
8. Liang Q, Yan X, Gu Y, Zhang K, Liang M, Lu S, Zheng X, Zhang Y (2015) Highly transparent triboelectric nanogenerator for harvesting water-related energy reinforced by antireflection coating. *Sci Rep* 5:1–7
9. Alam MM, Sultana A, Mandal D (2018) Biomechanical and acoustic energy harvesting from TiO₂ nanoparticle modulated PVDF nanofiber made high performance nanogenerator. *ACS Appl Energy Mater* 1:3103–3112
10. Yang Z, Zhang J, Kintner-Meyer MCW, Lu X, Choi D, Lemmon JP, Liu J (2011) Electrochemical energy storage for green grid. *Chem Rev* 111:3577–3613
11. Poullikkas A (2013) A comparative overview of large-scale battery systems for electricity storage. *Renew Sustain Energy Rev* 27:778–788
12. Luo X, Wang J, Dooner M, Clarke J (2015) Overview of current development in electrical energy storage technologies and the application potential in power system operation. *Appl Energy* 137:511–536
13. Ibrahim H, Ilinca A, Perron J (2008) Energy storage systems—characteristics and comparisons. *Renew Sustain Energy Rev* 12:1221–1250
14. Simon P, Gogotsi Y, Dunn B (2014) Where do batteries end and supercapacitors begin? *Science* 343:1210–1211
15. Yang M, Li Q, Zhang X, Bilotti E, Zhang C, Xu C, Gan S, Dang ZM (2022) Surface engineering of 2D dielectric polymer films for scalable production of high-energy-density films. *Prog Mater Sci* 128:100968
16. Simon P, Gogotsi Y (2008) Materials for electrochemical capacitors. *Nat Mater* 7:845–854
17. Sun Z, Ma C, Wang X, Liu M, Lu L, Wu M, Lou X, Wang H, Jia C (2017) Large energy density, excellent thermal stability, and high cycling endurance of lead-free BaZr_{0.2}Ti_{0.8}O₃ film capacitors. *ACS Appl Mater Interfaces* 9:17096–17101
18. Zhou M, Liang R, Zhou Z, Dong X (2018) Novel BaTiO₃-based lead-free ceramic capacitors featuring high energy storage density, high power density, and excellent stability. *J Mater Chem C* 6:8528–8537
19. Hu J, Zhang S, Tang B (2021) Rational design of nanomaterials for high energy density dielectric capacitors via electrospinning. *Energy Storage Mater* 37:530–555
20. Cheng R, Wang Y, Men R, Lei Z, Song J, Li Y, Guo M (2022) High-energy-density polymer dielectrics via compositional and structural tailoring for electrical energy storage. *iScience* 25, 104837
21. Gao F, Zhang K, Guo Y, Xu J, Szafran M (2021) (Ba, Sr)TiO₃/polymer dielectric composites—progress and perspective. *Prog Mater Sci* 121:100813
22. Huang X, Sun B, Zhu Y, Li S, Jiang P (2019) High-k polymer nanocomposites with 1D filler for dielectric and energy storage applications. *Prog Mater Sci* 100:187–225
23. Singh M, Apatal E, Samant S, Wu W, Tawade BV, Pradhan N, Raghavan D, Karima A (2022) Nanoscale strategies to enhance the energy storage capacity of polymeric dielectric capacitors: review of recent advances. *Poly Rev* 62:211–260

24. Zhang L, Liu Z, Lu X, Yang G, Zhang X, Cheng ZY (2016) Nano-clip based composites with a low percolation threshold and high dielectric constant. *Nano Energy* 26:550–557
25. Wanga H, Xie H, Wang S, Gao Z, Li C, Hu G, Xiong C (2018) Enhanced dielectric property and energy storage density of PVDF-HFP based dielectric composites by incorporation of silver nanoparticles-decorated exfoliated montmorillonite nanoplatelets. *Compos A* 108:62–68
26. Zh J-W, Zheng M-S, Fan B-H, Dang Z-M (2021) Polymer-based dielectrics with high permittivity for electric energy storage: a review. *Nano Energy* 89:106438
27. Sun L, Shi Z, Wang H, Zhang K, Dastan D, Sun K, Fan R (2020) Ultrahigh discharge efficiency and improved energy density in rationally designed bilayer polyetherimide-BaTiO₃/P(VDF-HFP) composites. *J Mater Chem A* 8:5750–5757
28. Wang Y, Yao MG, Ma R, Yuan QB, Yang DS, Cui B, Ma CR, Liu M, Hu DW (2020) Design strategy of barium titanate/polyvinylidene fluoride-based nanocomposite films for high energy storage. *J Mater Chem A* 8:884–917
29. Bouharras FE, Raihane M, Ameduri B (2020) Recent progress on core-shell structured BaTiO₃@polymer/fluorinated polymers nanocomposites for high energy storage: synthesis, dielectric properties and applications. *Prog Mater Sci* 113:100670
30. Feng Y, Zhou YH, Zhang TD, Zhang CH, Zhang YQ, Zhang Y, Chen QG, Chi QG (2020) Ultrahigh discharge efficiency and excellent energy density in oriented core-shell nanofiber-polyetherimide composites. *Energy Storage Mater* 25:180–192
31. Guo MF, Jiang JY, Shen ZH, Lin YH, Nan CW, Shen Y (2019) High-energy-density ferroelectric polymer nanocomposites for capacitive energy storage: enhanced breakdown strength and improved discharge efficiency. *Mater Today* 29:49–67
32. Marwat MA, Xie B, Zhu YW, Fan PY, Ma WG, Liu HM, Ashtar M, Xiao JZ, Salamon D, Samart C, Zhang HB (2019) Largely enhanced discharge energy density in linear polymer nanocomposites by designing a sandwich structure. *Compos Part A: Appl S* 121:115–122
33. Lu X, Zou XW, Shen JL, Zhang L, Jin L, Cheng ZY (2020) High energy density with ultrahigh discharging efficiency obtained in ceramic-polymer nanocomposites using a non-ferroelectric polar polymer as matrix. *Nano Energy* 70:104551
34. Zhou Y, Wang Q (2020) Advanced polymer dielectrics for high temperature capacitive energy storage. *J Appl Phys* 127:240902
35. Cheng S, Zhou Y, Hu J, He J, Li Q (2020) Polyimide films coated by magnetron sputtered boron nitride for high-temperature capacitor dielectrics. *IEEE T Dielect El In* 27:498–503
36. Li Q, Han K, Gadinski MR, Zhang G, Wang Q (2014) High energy and power density capacitors from solution-processed ternary ferroelectric polymer nanocomposites. *Adv Mater* 26:6244–6249
37. Tang H, Sodano HA (2013) Ultra high energy density nanocomposite capacitors with fast discharge using Ba_{0.2}Sr_{0.8}TiO₃ nanowires. *Nano Lett* 13:1373–1379
38. Huang X, Jiang P (2015) Core-shell structured high-k polymer nanocomposites for energy storage and dielectric applications. *Adv Mater* 27:546–554
39. Hu P, Shen Y, Guan YH, Zhang XH, Lin YH, Zhang QM, Nan CW (2014) Topological-structure modulated polymer nanocomposites exhibiting highly enhanced dielectric strength energy density. *Adv Funct Mater* 24:3172–3178
40. Zhang G, Li Q, Allahyarov E, Li Y, Zhu L (2021) Challenges and opportunities of polymer nanodielectrics for capacitive energy storage. *ACS Appl Mater Interfaces* 13:37939–37960
41. Jiang Y, Zhou M, Shen Z, Zhang X, Pan H, Lin YH (2021) Ferroelectric polymers and their nanocomposites for dielectric energy storage applications. *APL Mater* 9:020905
42. Shanmugasundram HPPV, Jayamani E, Soon KH (2022) A comprehensive review on dielectric composites: classification of dielectric composites. *Renew Sustain Energy Rev* 157:112075
43. Stark KH, Garton CG (1955) Electric strength of irradiated polythene. *Nature* 176:1225–1226
44. Hu J, Zhang S, Tang B (2021) 2D filler-reinforced polymer nanocomposite dielectrics for high-k dielectric and energy storage applications. *Energy Storage Mater* 34:260–281
45. Xiong X, Zhang Q, Zhang Z, Yang H, Tong J, Wen J (2021) Superior energy storage performance of PVDF-based composites induced by a novel nanotube structural BST@SiO₂ filler. *Composites: Part A* 145:106375

46. Jian G, Jiao Y, Meng Q, Wei Z, Zhang J, Yan C, Moon K, Wong C (2020) Enhanced dielectric constant and energy density in a BaTiO₃/polymer-matrix composite sponge. *Commun Mater* 1:1–12
47. Ren L, Yang L, Zhang S, Li H, Zhou Y, Ai D, Xie Z, Zhao X, Peng Z, Liao R, Wang Q (2021) Largely enhanced dielectric properties of polymer composites with HfO₂ nanoparticles for high-temperature film capacitors. *Compos Sci Technol* 201:108528
48. Dang Z, Yuan J, Zha J, Zhou T, Li S, Hu G (2012) Fundamentals, processes and applications of high-permittivity polymer–matrix composites. *Prog Mater Sci* 57:660–723
49. Yang W, Yu S, Sun R, Du R (2011) Nano- and microsize effect of CCTO fillers on the dielectric behavior of CCTO/PVDF composites. *Acta Mat* 59:5593–5602
50. Nelsont SO, You T-S (1990) Relationships between microwave permittivities of solid and pulverized Plastics. *J Phys D: Appl Phys* 23:346
51. Thomas S, Deepu VN, Mohanan P, Sebastian MT (2008) Effect of filler content on the dielectric properties of PTFE/ZnAl₂O₄–TiO₂ composites. *J Am Ceram Soc* 91:1971–1975
52. Dash S, Choudhary RNP, Kumar A, Goswami MN (2019) Enhanced dielectric properties and theoretical modeling of PVDF–ceramic composites. *J Mater Sci Mater Electron* 30:19309–19318
53. Hossain ME, Liu SY, O'Brien S, Li J (2014) Modeling of high-k dielectric nanocomposites. *Acta Mech* 225:1197–1209
54. Zhang C, Chi Q, Dong J, Cui Y, Wang X, Liu L, Lei Q (2016) Enhanced dielectric properties of poly(vinylidene fluoride) composites filled with nano iron oxide-deposited barium titanate hybrid particles. *Sci Rep* 6:1–9
55. Yamada T, Ueda T, Kitayama T (1982) Piezoelectricity of a high-content lead zirconate titanate polymer composite. *J Appl Phys* 53:4328–4332
56. Yu K, Niu Y, Zhou Y, Bai Y, Wang H (2013) Nanocomposites of surface-modified BaTiO₃ nanoparticles filled ferroelectric polymer with enhanced energy density. *J Am Ceram Soc* 96:2519–2524
57. Jayasundere N SV (1993) Dielectric constant for binary piezoelectric 0–3 composites. *J Appl Phys* 73:2462–2466
58. Hu H, Zhang F, Luo S, Chang W, Yue J, Wang CH (2020) Recent advances in rational design of polymer nanocomposite dielectrics for energy storage. *Nano Energy* 74:104844
59. Chen C, Xie Y, Liu J, Li J, Wei X, Zhang Z (2020) Enhanced energy storage capability of P(VDF-HFP) nanodielectrics by HfO₂ passivation layer: preparation, performance and simulation. *Compos Sci Technol* 188:107968
60. Tabhane GH, Giripunje SM, Kondawar SB (2021) Fabrication and dielectric performance of RGO-PANI reinforced PVDF/BaTiO₃ composite for energy harvesting. *Synth Met* 279:116845
61. Honga W, Pitike KC (2015) Modeling breakdown-resistant composite dielectrics. *Procedia IUTAM* 12:73–82
62. Sen ZH, Wang JJ, Lin Y, Nan CW, Chen LQ, Shen Y (2017) High-throughput phase-field design of high-energy-density polymer nanocomposites. *Adv Mater* 30:1704380
63. Niemeyer LP, Wiesmann HJ (1984) Fractal dimension of dielectric breakdown. *Phys Rev Lett* 52:1033
64. Yue D, Feng Y, Liu XX, Yin J-H, Zhang W-C, Guo H, Su B, Lei Q-Q (2022) Prediction of energy storage performance in polymer composites using high-throughput stochastic breakdown simulation and machine learning. *Adv Sci* 9:2105773
65. Wanga Z, Nelson JK, Hillborg H, Zhao S, Schadler LS (2013) Dielectric constant and breakdown strength of polymer composites with high aspect ratio fillers studied by finite element models. *Compos Sci Technol* 76:29–36
66. Bai H, Ge G, Shen B, Zhai J, Pan H (2020) Ultrahigh breakdown strength and energy density of polymer nanocomposite containing surface insulated BCZT@BN nanofibers. *Compos Sci Technol* 195:108209
67. Zhang T, Sun Q, Kang F, Wang Z, Xue R, Wang J, Zhang L (2022) Sandwich-structured polymer dielectric composite films for improving breakdown strength and energy density at high temperature. *Compos Sci Technol* 227:109596

68. Xu H, Xie C, Gou B, Wang R, Zhou J, Li L (2022) Core-double-shell structured BT@TiO₂@PDA and oriented BNNs doped epoxy nanocomposites with field-dependent nonlinear electrical properties and enhancing breakdown strength. *Compos Sci Technol* 230:109777
69. Huang X, Sun B, Zhua Y, Lib S, Jiang P (2019) High-k polymer nanocomposites with 1D filler for dielectric and energy storage applications. *Prog Mater Sci* 100:187–225
70. Rogti F, Ferhat M (2014) Maxwell Wagner polarization and interfacial charge at the multilayers of thermoplastic polymers. *J Electrostat* 72:91–97
71. Danikas MG (2010) On two nanocomposite models: differences, similarities and interpretational possibilities regarding Tsagaropoulos' model and Tanaka's model. *J Electr Eng* 61:241
72. Lewis TJ (2005) Interfaces: nanometric dielectrics. *J Phys D: Appl Phys* 38:202
73. Prateek TVK, Gupta RK (2016) Recent progress on ferroelectric polymer-based nanocomposites for high energy density capacitors: synthesis, dielectric properties, and future aspects. *Chem Rev* 116:4260–4317
74. Tiwari V, Srivastava G (2015) Structural, dielectric and piezoelectric properties of 0–3 PZT/PVDF composites. *Ceram Int* 41:8008–8013
75. Thomas P, Varughese KT, Dwarakanath K, Varma KBR (2010) Dielectric properties of Poly(vinylidene fluoride)/CaCu₃Ti₄O₁₂ composites. *Compos Sci Technol* 70:539–545
76. Fu J, Hou Y, Zheng M, Wei Q, Zhu M, Yan H (2015) Improving dielectric properties of PVDF composites by employing surface modified strong polarized BaTiO₃ particles derived by molten salt method. *Appl Mater Interfaces* 44:24480–24491
77. Kum-onsa P, Thongbai P (2020) Improved dielectric properties of poly(vinylidene fluoride) composites incorporating Na_{1/2}Y_{1/2}Cu₃Ti₄O₁₂ particles. *Mater Today Commun* 25:101654
78. Santos IA, Rosso JM, Cotica LF, Bonadio TGM, Freitas VF, Guo R, Bhalla AS (2016) Dielectric and structural features of the environmentally friendly leadfree PVDF/Ba_{0.3}Na_{0.7}Ti_{0.3}Nb_{0.7}O₃ 0–3 composite. *Curr Appl Phys* 16:1468–1472
79. Behera C, Choudhary RNP, Das PR (2017) Development of multiferroic polymer nanocomposite from PVDF and (Bi_{0.5}Ba_{0.25}Sr_{0.25})(Fe_{0.5}Ti_{0.5})O₃. *J Mater Sci: Mater Electron* 28:2586–2597
80. Ji SH, Cho JH, Jeong YH, Paik JH, Yun JD, Yun JS (2016) Flexible lead-free piezoelectric nanofiber composites based on BNT-ST and PVDF for frequency sensor applications. *Sensors and Actuators A* 247:316–322
81. Xie B, Wang T, Cai J, Zheng Q, Liu Z, Guo K, Mao P, Zhang H, Jiang S (2022) High energy density of ferroelectric polymer nanocomposites utilizing PZT@SiO₂nanocubes with morphotropic phase boundary. *J Chem Eng* 434:134659
82. Xie Z, Liu D, Xiao Y, Wang K, Zhang Q, Wu K, Fu Q (2022) The effect of filler permittivity on the dielectric properties of polymer-based composites. *Compos Sci Technol* 222:109342
83. Gonçalves R, Martins PM, Caparrós C, Martins P, Benelmekki M, Botelho G, Lanceros-Méndez S, Lasheras A, Gutierrez J, Barandiarán JM (2013) Nucleation of the electroactive β-phase, dielectric and magnetic response of poly(vinylidene fluoride) composites with Fe₂O₃ nanoparticles. *J Non-Cryst Solids* 361:93–99
84. Amoresi RAC, Felix AA, Botero ER, Falcão EA, Zaghet MA, Rinaldi AW (2015) Crystallinity, morphology and high dielectric permittivity of NiO nanosheets filling Poly(vinylidene fluoride). *Ceram Int* 41:14733–14739
85. Xu HP, Dang ZM (2007) Electrical property and microstructure analysis of poly(vinylidene fluoride)-based composites with different conducting fillers. *Chem Phys Lett* 438:196–202
86. Xu HP, Xie HQ, Yang DD, Wu YH, Wang JR (2011) Novel dielectric behaviors in PVDF-based semiconductor composites. *J Appl Polym Sci* 122:3466–3473
87. Dang ZM, Wang L, Yin Y, Zhang Q, Lei QQ (2007) Giant dielectric permittivities in functionalized carbon-nanotube/electroactive-polymer nanocomposites. *Adv Mater* 19:852–857
88. Wang L, Dang ZM (2005) Carbon nanotube composites with high dielectric constant at low percolation threshold. *Appl Phys Lett* 87:042903

89. Yousefi LX, Zheng Q, Shen X, Pothnis JR, Jia J, Zussman E, Kim JK (2013) Simultaneous in situ reduction, self-alignment and covalent bonding in graphene oxide/epoxy composites Nariman. *Carbon* 59:406–417
90. Stankovich S, Dikin DA, Dommett GHB, Kohlhaas KM, Zimney EJ, Stach EA, Piner RD, Nguyen ST, Ruoff RS (2006) Graphene-based composite materials. *Nature* 442:282–286
91. Yousefi N, Gudarzi MM, Zheng Q, Aboutalebi SH, Sharif F, Kim JK (2012) Self-alignment and high electrical conductivity of ultralarge graphene oxide–polyurethane nanocomposites. *J Mater Chem* 22:12709–12717
92. QiL LI, ChenS SD, ExarhosG J (2005) High-dielectric-constant silver-epoxy composites as embedded dielectrics. *Adv Mat* 17:1777–1781
93. Yousefi N, Sun X, Lin X, Shen X, Jia J, Zhang B, Tang B, Chan M, Kim JK (2014) Highly aligned graphene/polymer nanocomposites with excellent dielectric properties for high-performance electromagnetic interference shielding. *Adv Mater* 26:5480–5487
94. Guo D, Cai K, Deng P, Si G, Sun L, Chen F, Ning H, Jin L, Ma J (2020) Structure tailorable triple-phase and pure double-polar-phase flexible IF-WS₂@poly(vinylidene fluoride) nanocomposites with enhanced electrical and mechanical properties. *J Mater* 6:563–572
95. Jia Q, Huang X, Wang G, Diao J, Jiang P (2016) MoS₂ nanosheet superstructures based polymer composites for high-dielectric and electrical energy storage applications. *J Phys Chem C* 120:10206–10214
96. Wu W, Huang X, Li S, Jiang P, Toshikatsu T (2012) Novel three-dimensional zinc oxide superstructures for high dielectric constant polymer composites capable of withstanding high electric field. *J Phys Chem C* 116:24887–24895
97. Ji W, Deng H, Sun C, Fu Q (2019) Nickel hydroxide as novel filler for high energy density dielectric polymer composites. *Compos Sci Technol* 172:117–124
98. Wen F, Zhu C, Li L, Zhou B, Zhang L, Han C, Li W, Yue Z, Wu W, Wang G, Zhang S (2022) Enhanced energy storage performance of polymer nanocomposites using hybrid 2D ZnO@MoS₂ semiconductive nano-fillers. *J Chem Eng* 430:132676
99. Jing L, Li W, Gao C, Li M, Fei W (2022) Enabling high energy storage performance in PVDF-based nanocomposites filled with high-entropy oxide nanofiber. *Compos Sci Technol* 230:109783
100. Ji W, Deng H, Fu Q (2017) Heterogeneous filler distribution in polymeric capacitor films: an efficient route to improve their dielectric properties. *Compos Sci Technol* 151:131–138
101. Zeng J, Yan J, Li BW, Zhang X (2022) Improved breakdown strength and energy storage performances of PEI-based nanocomposite with core-shell structured PI@BaTiO₃ nanofillers. *Ceram Int* 48:20526
102. Hu J, Liu Y, Zhang S, Tang B (2022) Novel designed core–shell nanofibers constituted by single element-doped BaTiO₃ for high-energy–density polymer nanocomposites. *J Chem Eng* 428:131046
103. Li H, Wang L, Zhu Y, Jiang P, Huang X (2021) Tailoring the polarity of polymer shell on BaTiO₃ nanoparticle surface for improved energy storage performance of dielectric polymer nanocomposites. *Chin Chem Lett* 32:2229–2232
104. Pan X, Wang M, Qi X, Zhang N, Huang T, Yang J, Wang Y (2020) Fabrication of sandwich-structured PPy/MoS₂/PPy nanosheets for polymer composites with high dielectric constant, low loss and high breakdown strength. *Compos A* 137:106032
105. Li Z, Liu F, Li H, Ren L, Dong L, Xiong C, Wang Q (2019) Largely enhanced energy storage performance of sandwich-structured polymer nanocomposites with synergistic inorganic nanowires. *Ceram Int* 45:8216–8221
106. Luo W, Xu L, Zhang G, Zhou L, Li H (2021) Sandwich-structured polymer nanocomposites with Ba_{0.6}Sr_{0.4}TiO₃ nanofibers networks as mediate layer inducing enhanced energy storage density. *Compos Sci Technol* 204:108628
107. Wang Y, Hou Y, Deng Y (2017) Effects of interfaces between adjacent layers on breakdown strength and energy density in sandwich-structured polymer composites. *Compos Sci Technol* 145:71–77